Removal of lead ion from environmental samples using modified glass nanoparticles

Saba Arjmandpour[a], Homayon Ahmad Panahi[b],*

[a]Department of Chemistry, Karaj Branch, Islamic Azad University, Alborz, Iran, Tel. +989125654147; email: saba.arj67@yahoo.com
[b]Department of Chemistry, Central Tehran Branch, Islamic Azad University, Tehran, Iran, Tel. & Fax: +982144164539;
email: h.ahmadpanahi@iauctb.ac.ir

ABSTRACT

Allylamine and N,N-dimethylacrylamide were graft-polymerized to modified silylate glass nanoparticles with 3-mercaptopropyltrimethoxysilane. Then, the grafted polymeric chines were modified with bromoacetic acid. The final grafted nanoglass was characterized through Fourier transform infra-red spectroscopy, elemental analysis, scanning electron microscopy, and transmission electron microscopy. The trace amounts of Pb (II) ions from milk, human plasma, and environmental water samples were successfully removed by grafted nanoglass, which shows the chelating sites on nanosorbent were suitably accessible for Pb (II) in the sample. The optimal pH value for Pb (II) adsorption was measured to be 5.5 in batch mode. The adsorption capacity of the sorbent was obtained to be 26.7 mg g^{-1} for Pb (II) under the optimal conditions. For designing the equilibrium data of the sorption process, the Temkin, Langmuir, and Freundlich models were applied as the adsorption isotherms with the constants of 3.97 (J mol^{-1}), 0.34 (L mg^{-1}), and 10.1 (mg g^{-1}) (L mg^{-1})$^{1/n}$ under the optimum pH value of 5.5 at ambient temperature, respectively.

Keywords: Polymer grafting; Lead; Glass nanoparticles; Environmental samples

1. Introduction

Heavy metals are toxic and can cause damage to some vital factors in human body at high concentrations. Toxic heavy metals like Pb, Cu, Ni, Cd, and Hg can enter the body via food and breathing or absorption through the skin [1–5]. One of these toxic heavy metals is lead, which is distributed in the environment through different chemical pollutants and can eventually enter the food chain. It tends to accumulate in living organisms and cause various life-threatening illnesses, such as anemia, kidney and brain damage, paralysis, miscarriage, and behavioral disturbances, when accumulated in the bone marrow [6–8]. Hence, there is a great need to find practical procedures for reducing lead from water and protect the environment.

Many attempts have been recently focused on repulsing these threats by researchers, which have resulted in the development of a variety of separation procedures for removing this toxic metal from aqueous solutions. These procedures include chemical precipitation [9], ion exchange [10], adsorption [11,12], membrane filtration [13], and coagulation–flocculation [14]. Among these approaches, adsorption process is commonly applied because of its simplicity, feasibility, and high selectivity and efficiency. Accordingly, nanoadsorbents have been highly considered for their special properties such as large surface area and high adsorption capacity [15]. Glass nanoparticles (NPs) have shown to be advantageous due to their physical and chemical stabilities, non-toxicity, easy availability, simple preparation, and low cost [16].

A highly sensitive and selective technique is required for the determination of lead adsorption amount. There are many instrumental techniques, such as flame atomic absorption spectrometry (FAAS) [17], inductively coupled plasma mass spectrometry [18], and graphite-furnace atomic-absorption

---

* Corresponding author.

spectrometry [19], but FAAS is preferred because of its simplicity and cost efficiency.

Graft polymerization is a common modification method for preparing a tailored surface with desired functions [20]. The grafted polymer chains on the reactive sites of solid surfaces change the interfacial properties of the substrate, thus providing a method for controlling the interactions between surfaces and solutes [21,22]. Grafting can be carried out by either "grafting-from" or "grafting-to" procedures. In the "grafting-from" approach, a substrate is treated to produce immobilized initiators followed by polymerization, while in the "grafting-to" method, functionalized monomers are employed to react with the backbone polymer and generate the grafted one [23].

In the present study, graft polymerization of N,N-dimethylacrylamide (DMAA) and a functional monomer containing the metal-chelating group of allylamine (AA) onto glass NP surfaces silylated with 3-mercaptopropyltrimethoxysilane (3-MPTMS) and finally modified with bromoacetic acid (BAA) was reported. The aim of this work was to study the feasibility of Pb (II) ion adsorption from environmental water samples onto glass NPs grafted by DMAA and AA and modified with BAA (GN-DAB). The adsorption of trace lead onto GN-DAB surface was evidenced and the amount of lead remaining in the eluate was determined via FAAS.

2. Experimental procedure

2.1. Instruments

The metal ions were determined by using a flame atomic absorption spectrometer (Varian Model AA240, Palo Alto, CA, USA) in the air–acetylene flame at the flow rates of 8 and 1.7 L min^{-1} for air and acetylene, respectively. In addition, an inductively coupled plasma-optical emission spectrometer (Varian Model 715-ES, Santa Clara, CA, USA) was applied. PH adjustments were done by using a pH meter (Model WTW 7110, Weilheim, Germany). A Perkin-Elmer spectrometer (Model 100, Shelton, USA) was employed to record the infra red (IR) spectra. The elemental analysis (EA) of the functionalized sorbent was performed by using a Costech elemental analyzer (Model ECS 4010, Valencia, CA, USA). The scanning electron microscopy (SEM) micrographs were acquired through a scanning electron microscope (KYKY Model EM3200, Zhongguancun, Beijing, China). The transmission electron microscopy (TEM) was conducted by using a Philips transmission electron microscope (Model CM120, Amsterdam, the Netherlands). Surface areas were done using the Brunauer–Emmentt–Teller (BET) method (BElSORP Mini, Microtrac Bel Corp Company, Osaka, Japan). The nanodimensional coverslip powder was prepared by using a Fritsch Pulverisette 6 classic line Planetary Mono-Mill (Idar-Oberstein, Germany).

2.2. Reagents and solutions

3-MPTMS, anhydrous toluene, 2,2'-Azobis (2-methylpropionitrile) (AIBN), AA, DMAA, and BAA were purchased from Aldrich (Steinheim, Germany). The impurities inhibiting polymerization were removed by purifying 2,2'-azobis(2-methylpropionitrile). The applied ethanol, ethylenediaminetetraacetic acid, $NaHCO_3$, K_2HPO_4, KH_2PO_4, CH_3COONa, CH_3COOH, HNO_3, and HCl were products of Merck (Darmstadt, Germany). To prepare the reagent solutions, the chemical compounds of analytical grade were utilized without further purification. The stock solutions of Co (II), Cd (II), Al (III), Ni (II), Zn (II), Ag (I), Cu (II), Fe (III) (10, 50, and 100 mg L^{-1}), and Pb (II) (1,000 mg L^{-1}) were prepared by dissolving appropriate amounts of $CoSO_4 \cdot 8H_2O$, $CdSO_4$, $Al (NO_3)_3 \cdot 9H_2O$, $NiSO_4 \cdot 6H_2O$, $Zn (NO_3)_2 \cdot 6H_2O$, $AgNO_3$, $CuSO_4 \cdot 5H_2O$, $FeSO_4 \cdot 7H_2O$, and $Pb (NO_3)_2$ in deionized water. To optimize the pH values of the solutions, 10 mL of 0.01 M acetic acid/acetate buffer or 0.01 M phosphate buffer was used within the pH ranges of 3.5–6.5 and 7–7.5 whenever suitable, respectively.

2.3. Synthesis of the GN-DAB

At first, some glass coverslips were provided and powdered using mortar as much as possible. Then, their nanodimensional sizes were prepared by using a planetary mono-mill.

2.3.1. Modification of glass NPs with 3-MPTMS

First, 2.5 mL of 3-MPTMS was added to 47.5 mL of anhydrous toluene. Then, 3 g of glass NPs was added to the mixture. Afterwards, the mixture was refluxed in an oil bath at 70°C–80°C for 3 d. Upon completion of the reaction, the slurry was filtered and washed with 30 mL of anhydrous toluene. Finally, the washed glass NPs were dried in a desiccator over dry calcium chloride.

2.3.2. Graft polymerization

At this stage, 10 mL of AA, 2 mL of DMAA, and 30 mL of ethanol (as a solvent) were added to the silylated glass NPs. The mixture was stirred under nitrogen atmosphere for 5 min. Nitrogen atmosphere was needed to exclude oxygen, which could waste the free radicals and stop the polymerization process. Then, 0.1 g of AIBN was added to the degassed polymerization mixture and the slurry was refluxed on a water bath at 65°C–70°C under nitrogen atmosphere for 7 h. After filtering the grafted glass NPs and washing them with 40 mL of ethanol, they were dried in a desiccator over dry calcium chloride.

2.3.3. Modification with BAA

To this aim, 2 g of BAA was dissolved in 100 mL of 0.1 M sodium bicarbonate solution, to which the grafted NPs were added. The mixture was powerfully stirred at ambient temperature for 6 h. When the reaction was finished, the mixture was washed with water, 50 mL of 0.1 M $NaHCO_3$, and again with water under stirring and then dried under ambient conditions. A summary of the applied methodology for GN-DAB synthesis is presented in Fig. 1. GN-DAB characterizations were performed through Fourier transform infra-red (FTIR) spectroscopy, EA, SEM, and TEM.

2.4. Batch method of Pb (II) adsorption

Batch adsorption experiments were performed using 100 mL of a sample solution including 0.5 μg mL^{-1} of Pb (II),
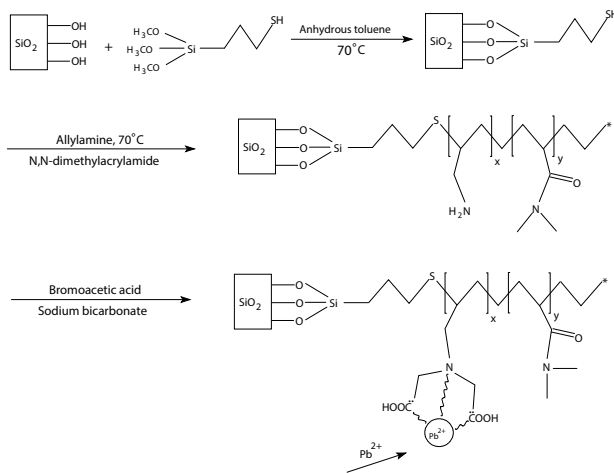
Fig. 1. Schematic presentation of synthesis of GN-DAB.

which was then transferred into a beaker. Adjustment of the optimal pH value of the solution was followed. After adding 0.1 g of GN-DAB to the solution, it was stirred within an optimum time. Upon filtration of the sorbent, Pb (II) ion concentration in the solution was determined via FAAS.

2.5. Isotherm studies

In this step, 50-mL Pb (II) solutions were prepared at their initial concentrations of 5–100 µg mL^{-1} and pH values of 5.5 (adjusted by adding 0.01 M acetate buffer) in some beakers and 0.05 g of GN-DAB was added to them. The beakers were then stirred at ambient temperature for 3 h. After filtering the sorbent, the final lead ion concentration

was obtained through FAAS. The amount of Pb (II) absorbed onto GN-DAB at equilibrium (mg g^{-1}) was determined by the following equation:

$$q_e = \frac{(C_0 - C_e)V}{W} \tag{1}$$

where C_0 and C_e (mg L^{-1}) indicate lead initial and equilibrium concentrations, respectively; V (L) denotes the solution volume and W (g) stands for GN-DAB mass.

3. Results and discussion

3.1. GN-DAB characterizations

3.1.1. IR spectrum analysis

In the FTIR spectrum of GN-DAB, the peaks at 3,442 and 1,069 cm^{-1} can be attributed to the stretching vibrations of O-H and Si-O groups, respectively. The presence of C-O, C=O, and aliphatic C-H groups in Fig. 2 for the present adsorbent were proved by spectral bands at 1,152, 1,803, 2,230 cm^{-1}, respectively [24]. Presence of these peaks suggests that the glass nanoparticles are functionalized properly and confirms the presence of respective groups at the surface of the nanoparticles.

3.1.2. Elemental Analysis

The EA results of C, H, N, and S for GN-DAB were 1.75%, 0.14%, 0.25%, and 0.23%, respectively. These results corroborated the presence of the mentioned elements in the synthesized adsorbent and demonstrated the successful polymerization and modification of GN-DAB.
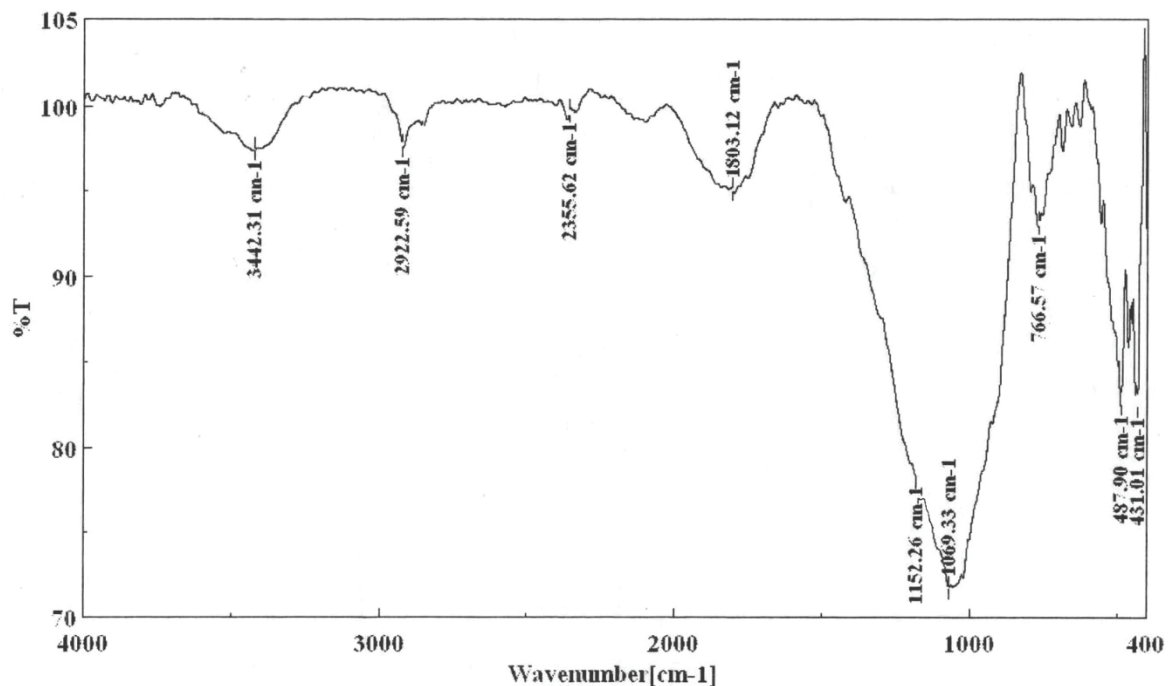

Fig. 2. FTIR spectrum of GN-DAB.

3.1.3. SEM analysis

The structural properties and surface morphologies of the GN-DAB beads were investigated through SEM (Fig. 3(a)). As can be seen in this figure, GN-DAB is in the shape of agglomerated granular grains. These NPs are in the size range of 10–100 nm, most of which have a diameter of 20–40 nm.

3.1.4. TEM analysis

The TEM micrograph (Fig. 3(b)) showed and confirmed the spherical and agglomerated structures of the NPs.
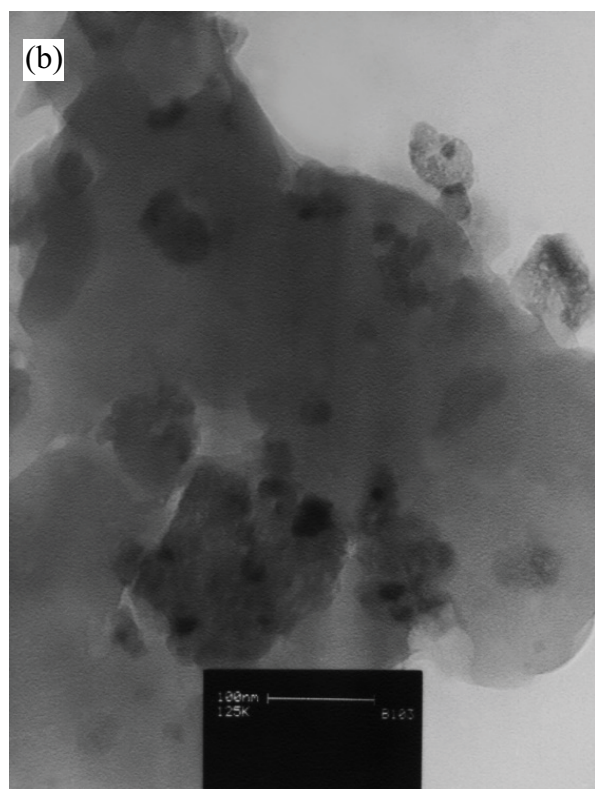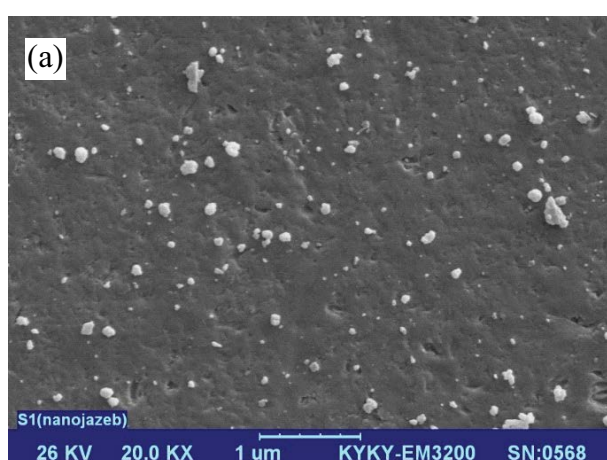

Fig. 3. (a) SEM and (b) TEM image of GN-DAB.

3.2. Metal sorption

The suggested mechanism for the adsorption of Pb (II) by grafted nanoglass is demonstrated in Fig. 1. With the best of our knowledge, two types of interactions are involving for Pb (II) adsorption: (i) the first one is electrostatic interactions between the positive lead ions and negative oxygen in carboxylic acid, so Pb (II) ions can be easily exchange with H+ in this groups and (ii) the coordinate bonding between nitrogen and oxygen in iminodiacetic acid and Pb (II) ions as shown in Fig. 1.

The adsorption behavior of Pb (II) on GN-DAB surface was investigated over the pH range of 3.5–7.5 via batch equilibration technique. The results are displayed in Fig. 4. The maximum adsorption for GN-DAB was obtained at a pH value of 5.5. As can be seen, the best adsorption has occurred within moderate acidic pH ranges, thus indicating the highest interaction of Pb (II) ions and the adsorbent and proper chelation of Pb (II) ions by the adsorbent. Since the glass powder was found to be dissolved in the basic pH ranges and Pb (II) ions were deposited as Pb $(OH)_2$, there was no need to test higher pH ranges in the current study. The adsorption percentage of Pb (II) vs. contact time is demonstrated in Fig. 5. As can be seen, maximum adsorption has been accomplished during 10 min of good accessibility to the chelating sites in GN-DAB for interacting with Pb (II).

3.3. Adsorption isotherms

In the present research, the different models of Langmuir, Freundlich, and Temkin isotherms were employed to assess the studied adsorbent affinity for removing Pb (II) ions from the aqueous solutions.

The Langmuir isotherm assumes the adsorption at the surface monolayer coverage with a finite number of identical and equivalent adsorption sites. The related equation [25] can be given as follows:

$$q_e = q_{max} \times \frac{K_L . C_e}{\left(1 + K_L . C_e\right)}$$ (2)

where q_{max} (mg g^{-1}) represents the maximum adsorption capacity of the adsorbent at the monolayer surface; C_e (mg L^{-1}) demonstrates the equilibrium concentration and K_L (L mg^{-1}) displays the Langmuir constant related to the
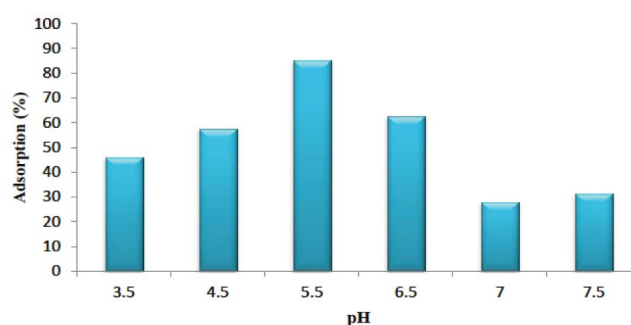

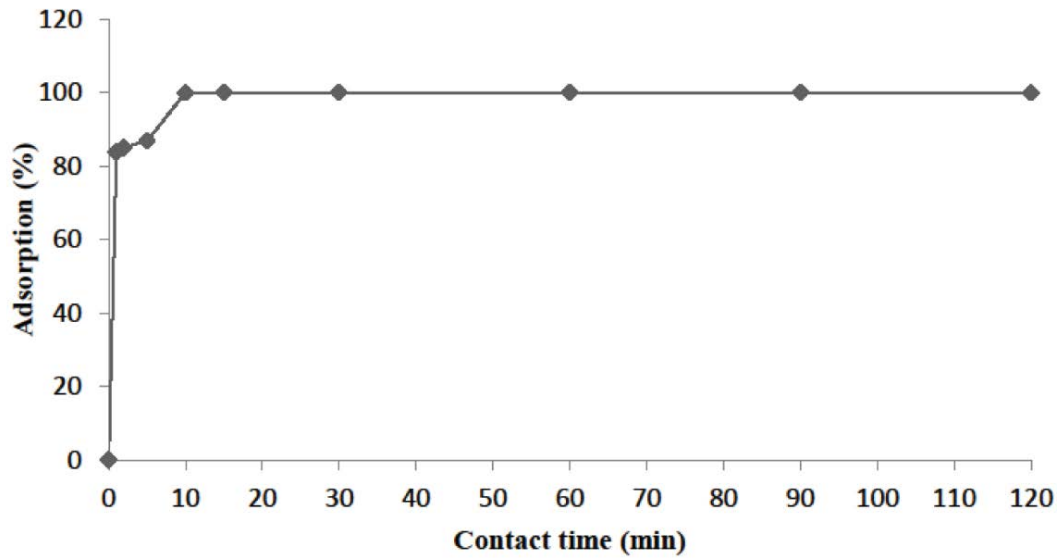Fig. 4. Effect of pH on adsorption of Pb (II) ions on GN-DAB.

Fig. 5. Effect of contact time on adsorption of Pb (II) ions on GN-DAB.

affinity and energy of the binding sites. The linear form of this model is exhibited as follows:

$$\frac{C_e}{q_e} = \left(\frac{1}{q_{max}} \times K_L \right) + \left(\frac{C_e}{q_{max}} \right) \tag{3}$$

A plot of C_e/q_e vs. C_e enables the determination of the constants from the slope and intercept. Fitting of the experimental data into the Langmuir isotherm model suggested the homogeneous binding sites of GN-DAB and the monolayer adsorption of Pb (II) onto its outer surface. According to this isotherm curve, the isotherm parameters of the Langmuir model calculated from Eq. (3) are listed in Table 1.

The Langmuir isotherm can be expressed in terms of a dimensionless constant separation factor called R_L, which is defined as follows:

$$R_L = \frac{1}{\left(1 + K_{L.}.C_0 \right)} \tag{4}$$

R_L value of 0.028 is in the range of 0–1 at pH = 5.5, which represents the desirable description of lead adsorption phenomenon by the Langmuir theory.

As an empirical equation, the Freundlich isotherm is used to depict adsorption on a heterogeneous surface and the interaction between the adsorbed molecules, which can be expressed as follows [25]:

$$q_e = K_F \times C_e^{1/n} \tag{5}$$

where K_F (mg g^{-1})(L mg^{-1})$^{1/n}$ is the Freundlich constant related to the bonding energy and $1/n$ is the heterogeneity factor, which can be calculated from the slope and intercept of the linear plot (Eq. (6)) according to $\ln q_e$ vs. $\ln C_e$ as follows:

$$\ln q_e = \ln K_F + \frac{1}{n} \ln C_e \tag{6}$$

Table 1
Isotherm parameters obtained by using linear method

Isotherm				
Langmuir	q_{max} (mg g^{-1})	K_L (L mg^{-1})	R_L	R^2
	26.70	0.34	0.03	0.9979
Frendlich		K_F (mg g^{-1}) (L mg^{-1})$^{1/n}$	n	R^2
		10.10	4.23	0.9603
Temkin	A (L g^{-1})	B (J mol^{-1})	b (J mol^{-1})	R^2
	11.10	3.97	624.074	0.9699

The Freundlich equation could describe the relation between Pb (II) concentration on the adsorbent and in the liquid. By increasing Pb (II) concentration in the liquid, its concentration on the adsorbent was seen to be enhanced.

The Temkin equation was indicative of the linearly reduced adsorption heat of all the molecules by increasing the adsorbate layer coverage on the adsorbent surface. The related isotherm is represented as follows [25]:

$$q_e = \left(\frac{RT}{b}\right) \ln AC_e \tag{7}$$

which can be linearized as this:

$$q_e = B \ln A + B \ln C_e \tag{8}$$

where and b (J mol^{-1}) is the Temkin constant relevant to the adsorption heat, R represents the gas constant equal to 8.314 J mol^{-1} K^{-1}, A (L g^{-1}) demonstrates the Temkin isotherm constant relevant to adsorption capacity, and T (K) denotes the absolute temperature in degrees Kelvin. Constants A and B can be calculated from the linear plots of q_e vs. ln C_e. The Temkin parameters obtained from Eqs. (7) and (8) are presented in Table 1.

3.4. BET Isotherm

The characterization of the N$_2$ adsorption–desorption was employed to further investigate the porous nature of the GN-DAB. The sample exhibited type IV isotherms with a distinct hysteresis loop according to the International Union of Pure and Applied Chemistry (IUPAC) standards, suggesting a typical mesoporous structure of them. The BET surface areas of GN-DAB were 0.22 m^2 g^{-1}. Total pore volume ($p/p_0 = 0.990$) was 6.9×10^{-4} cm^{-3} g^{-1}. Mean pore diameter was obtained 12.7 nm.

3.5. Adsorption kinetics

Pseudo-first-order (PFO) equation is one of the most popular and empirical models for adsorption kinetics presented by Lagergren.

The linear form of PFO can be given as follows:

$$\ln(q_e - q_t) = \ln(q_e) - \left(\frac{k_1 t}{2.303}\right) \tag{9}$$

where q_e and q_t (mg g^{-1}) are the adsorption capacity at equilibrium and time t (min), respectively and k_1 (min^{-1}) is the PFO rate constant.

Another well-known kinetic model is pseudo-second-order (PSO) equation with this equation:

$$\frac{t}{q_t} = \left(\frac{1}{k_2 q_e^2}\right) + \left(\frac{t}{q_e}\right) \tag{10}$$

where k_2 (mg g^{-1} min^{-1}) is the PSO rate constant.

The last considered kinetic model is intraparticle diffusion (ID) model with Eq. (11):

$$q_t = k_p t^{0.5} + A \tag{11}$$

where k_p is the ID rate constant. A (mg g^{-1}) is a constant that gives an indication of the thickness of the boundary layer.

Kinetic parameters of the models are given in Table 2. It is obvious from Table 2 that the highest correlation coefficients ($r^2 = 1$) are related to PSO; thus, it can be concluded that PSO model is suitable to describe the kinetic experimental data. The low values of rate constant ($k_2 = 0.0032$) suggested that the adsorption rate of Pb (II) by GN-DAB would decrease with the increase in time and this rate could be proportional to the number of unoccupied sites on the GN-DAB.

3.6. The effect of foreign ions

The probable interference of some metal ions with the adsorption behavior of Pb (II) ions at a concentration of 10 mg L^{-1} was studied. The interference was found to occur because of the competition of other heavy metal ions with lead ion for the chelating sites. The results are listed in Table 3. As shown in this Table, Cu (II), Co (II), and Cd (II) are the most effective ions on Pb (II) adsorption onto GN-DAB. The effects of the other foreign ions mentioned at the given concentrations are insignificant. As demonstrated by the results, the mentioned ions can interfere with Pb (II) adsorption onto GN-DAB. Thus, GN-DAB cannot be selectively operated for the adsorption of Pb (II) ions in the environmental water samples.

3.7. Application of the proposed method

The experiments aimed at testing Pb (II) removal from the environmental water samples by using GN-DAB. Different water and milk samples from the Persian Gulf (Boshehr Province, Iran), Vafs Spring (Markazi Province, Iran), Aghsu (Golestan Province, Iran), and Haraz (Mazandaran Province, Iran) rivers were collected. 2 mL of concentrated hydrochloric acid was added to the prepared milk samples and centrifuged to separate their proteins via flocculation. Adjustments of the optimum pH values of the samples were followed. The batch method of GN-DAB coupled with FAAS

Table 2
Constant of kinetic models for adsorption of Pb (II) onto GN-DAB

Isotherm	Parameters	
Pseudo-first-order	k_1 (min^{-1})	0.38
	q_e (mg g^{-1})	2.2
	r^2	0.9326
pseudo-second-order	k_2 (g mg^{-1} min^{-1})	0.0032
	q_e (mg g^{-1})	17.5
	r^2	1
Intraparticle diffusion	k_p	1.36
	A	12.98
	r^2	0.9876

Table 3
Effect of other ions on sorption of Pb (II)

Interfering ions	Amount of adsorbed Pb (II) (mg L^{-1})	Loss adsorption (%)
–	10	–
Cu^{2+}	6.56	34.4
Ni^{2+}	8.06	19.4
Co^{2+}	6.11	38.9
Ag^+	10	–
Fe^{3+}	8.88	11.2
Zn^{2+}	7.43	25.7
Cd^{2+}	5.25	47.5
Al^{3+}	7.82	21.8

was applied to remove Pb (II) ions from the samples. Since the trace amounts of lead were detected in the water samples, 250 mL of them was spiked with Pb (II) (0.01 mg) to be

then utilized in the current procedure. They showed to be applicable to lead removal as displayed in Table 4.

Also, the removal of Pb (II) ions from human serum was studied. Since no Pb (II) ions were detected in the serum, 25 mL of the serum was spiked with 0.01 mg of Pb (II) to be used in the procedure. Since high concentrations of plasma samples can cause obstruction of the capillary tube of FAAS instrument, the plasma samples were determined via inductively coupled plasma optical emission spectrometry (ICP-OES; Table 4).

3.8. Comparison of the proposed approach with other methods

The proposed procedure was compared with the previously reported studies on lead removal through various methods. The maximum adsorption capacities of the adsorbents are represented in Table 5. This table shows that the adsorption capacity obtained from the present adsorbent is comparable to or better than those of some previously reported techniques. The new procedure was successfully applied for the analysis of trace lead ions in the environmental samples.

Table 4
Results for Pb (II) removal from environmental water samples

	Persian golf	Vafs spring	Aghsou river	Haraz river	Milk	Plasma
Found (without spiking of Pb (II)) (mg L^{-1})	0.48	0.03	0.04	0.12	0.29	N.D.
Added Pb (II) (mg L^{-1})	0.1	0.1	0.1	0.1	0.1	0.1
Found Pb (II) after spiking of Pb (II) (mg L^{-1})	0.58	0.13	0.14	0.22	0.39	0.1
Adsorption (%)	82.1	87	91.5	88.3	70.1	91.9
Standard deviation	0.005937	0.000757	0.000208	0.001493	0.00526	0.000212
Relative standard deviation (%)*	5.7	4.5	1.7	5.8	4.5	2.6

*For three determination.

Table 5
Comparison of the maximum adsorption capacity with some literatures

Adsorbent	q_{max} (mg g^{-1})	References
Activated carbon	13.05	[26]
Silica gel/Gallic acid	12.63	[27]
Peels of banana	2.18	[28]
Acid-treated maize tassel biomass	37.31	[29]
1:9 MPTMS:Tetraethyl orthosilicate (cashew nut shell liquid)	22.7	[30]
Walnut shell	31.23	[31]
Apple pomace	16.39	[32]
Gallic acid-modified silica gel	12.63	[33]
Nanometer titanium dioxide immobilized on silica gel	3.16	[34]
Dithizone-modified TiO_2 nanoparticles	5.8	[35]
Fig sawdust activated carbon	80.6	[36]
Surfactant-assisted nanocomposite cation exchanger	351.9	[37]
GN-DAB	26.7	Present study

4. Conclusion

In the present research, a new grafted nanoglass was synthesized with organic chelating ligands for the removal of lead ions from some biological and environmental water samples. The present nanoadsorbent may be considered as a useful material due to its simplicity and economical aspects. Our study demonstrated its merits of high sorption capacity, fast sorption, and also chemical stability. The equilibrium data were found to be fitted with the Langmuir isotherm with an adsorption capacity of 26.7 mg g^{-1}. The R_L value reflected the desirable potential of the adsorbent for Pb (II) from water sample solutions. This adsorbent can be applied to remove the trace amounts of lead ions from biological and environmental water samples through the combined methods of FAAS and ICP-OES with satisfactory results.

Symbols

A	—	Temkin isotherm constant relevant to adsorption capacity, L g^{-1}
b	—	Temkin isotherm constant, J mol^{-1}
B	—	Temkin constant relevant to the adsorption heat, J mol^{-1}
C_0	—	Initial concentration, mg L^{-1}
C_e	—	Equilibrium concentration, mg L^{-1}
K_F	—	Freundlich isotherm constant, (mg g^{-1}) (L mg^{-1})$^{1/n}$
K_L	—	Langmuir isotherm constant, L mg^{-1}
q_e	—	The amount of equilibrium adsorption, mg g^{-1}
q_{max}	—	Maximum adsorption capacity, mg g^{-1}
R	—	Universal gas constant, J mol^{-1} K^{-1}
R_L	—	Dimensionless constant separation factor
T	—	Absolute temperature, K
V	—	Solution volume, L
W	—	Mass, g

References

[1] M.H. Mashhadizadeh, Z. Karami, Solid phase extraction of trace amounts of Ag, Cd, Cu, and Zn in environmental samples using magnetic nanoparticles coated by 3-(trimethoxysilyl)-1-propantiol and modified with 2-amino-5-mercapto-1,3,4-thiadiazole and their determination by ICP-OES, J. Hazard. Mater., 190 (2011) 1023–1029.

[2] R. Bushra, Mu. Naushad, R. Adnan, Z.A. ALOthman, M. Rafatullah, Polyaniline supported nanocomposite cation exchanger: synthesis, characterization and applications for the efficient removal of Pb^{2+} ion from aqueous medium, J. Ind. Eng. Chem., 21 (2015) 1112–1118.

[3] R. Bushra, Mu. Naushad, G. Sharma, A. Azam, Z.A. ALOthman, Synthesis of polyaniline based composite material and its analytical applications for the removal of highly toxic Hg^{2+} metal ion: Antibacterial activity against *E. coli*, Korean J. Chem. Eng., 34 (2017) 1970–1979.

[4] Mu. Naushad, T. Ahamad, B.M. Al-Maswari, A.A. Alqadami, S.M. Alshehri, Nickel ferrite bearing nitrogen-doped mesoporous carbon as efficient adsorbent for the removal of highly toxic metal ion from aqueous medium, Chem. Eng. J., 330 (2017) 1351–1360.

[5] H.A. Panahi, E. Mottaghinejad, A.R. Badr, E. Moniri, Synthesis, characterization, and application of amberlite XAD-2-salicylic acid- iminodiacetic acid for lead removal from human plasma and environmental samples, J. Appl. Polym. Sci., 121 (2011) 1127–1136.

[6] M. Irania, M. Amjadib, M.A. Mousavian, Comparative study of lead sorption onto natural perlite, dolomite and diatomite, Chem. Eng. J., 178 (2011) 317–323.

[7] Residential lead hazards standards_ TSCA section 403, Environmental Protection Agency, EPA, 2005.

[8] V.K. Gupta, I. Ali, Removal of lead and chromium from wastewater using bagasse fly ash—a sugar industry waste, J. Colloid Interface Sci., 271 (2004) 321–328.

[9] K. Prasad, P. Gopikrishna, R. Kala, T.P. Rao, G.R.K. Naidu, Solid phase extraction vis-à-vis coprecipitation preconcentration of cadmium and lead from soils onto 5,7-dibromoquinoline-8-ol embedded benzophenone and determination by FAAS, Talanta, 69 (2006) 938–945.

[10] E. Pehlivan, T. Altun, Ion-exchange of Pb^{2+}, Cu^{2+}, Zn^{2+}, Cd^{2+}, and Ni^{2+} ions from aqueous solution by Lewatit CNP 80, J. Hazard. Mater., 140 (2007) 299–307.

[11] N. Chiron, R. Guilet, E. Deydier, Adsorption of Cu (II) and Pb (II) onto a grafted silica: isotherms and kinetic models, Water Res., 37 (2003) 3079–3086.

[12] H. Ahmad panahi, J. Morshedian, N. Mehmandost, E. Moniri, I.Y. Galaev, Grafting of poly[1-(N,N-bis-carboxymethyl) amino-3-allylglycerol-co-dimethylacrylamide] copolymer onto siliceous support for preconcentration and determination of lead (II) in human plasma and environmental samples, J. Chromatogr. A., 1217 (2010) 5165–5172.

[13] M.H.M. Reis, V.L. Cardoso, Biodiesel production and purification using membrane technology, Membrane Technologies for Biorefining, Elsevier, 2016, pp. 289–307.

[14] G. Han, C.Z. Liang, T.S. Chung, M. Weber, C. Staudt, C. Maletzko, Combination of forward osmosis (FO) process with coagulation/flocculation (CF) for potential treatment of textile wastewater, Water Res., 91 (2016) 361–370.

[15] G.Q. Lu, X.S. Zhao, Nanoporous Materials,Science and Engineering, World Science, Imperial College Press, London, 2004.

[16] E.F. Vasant, P. Van Der Voort, K.C. Vrancken, Characterization and Chemical Modification of the Silica Surface, 1st ed., Elsevier Science, The Netherlands, 93, 1995.

[17] W.I. Mortada, I.M.M. Kenawy, A.M. Abdelghany, A.M. Ismail, A.F. Donia, K.A. Nabieh, Determination of Cu^{2+}, Zn^{2+} and Pb^{2+} in biological and food samples by FAAS after preconcentration with hydroxyapatite nanorods originated from eggshell, Mater. Sci. Eng. C, 52 (2015) 288–296.

[18] R. Clough, H. Sela, A. Milne, M.C. Lohan, S. Tokalioglu, P.J. Worsfold, Uncertainty contributions to the measurement of dissolved Co, Fe, Pb and V in seawater using flow injection with solid phase preconcentration and detection by collision/reaction cell-quadrupole ICP-MS, Talanta, 133 (2015) 162–169.

[19] H.M. Jiang, Z.P. Yan, Y. Zhao, X. Hu, H.Z. Lian, Zincon-immobilized silica-coated magnetic Fe$_3$O$_4$ nanoparticles for solid-phase extraction and determination of trace lead in natural and drinking waters by graphite furnace atomic absorption spectrometry, Talanta, 94 (2012) 251–256.

[20] Z.K. Xu, X.J. Huang, L.S. Wan, Surface Engineering of Polymer Membranes, Springer, Berlin and Heidelberg, 2009.

[21] M. Chaimberg, R. Parnas, Y.J. Cohen, Graft polymerization of polyvinylpyrrolidone onto silica, J. Appl. Polym. Sci., 37 (1989) 2921–2931.

[22] F. Rodriguez, Principles of Polymer Systems, 2nd ed., McGraw-Hill, New York, 1982.

[23] Bhattacharya, J.W. Rawlins, P. Ray, Polymer Grafting and Crosslinking, John Wiley & Sons Inc., New Jersey, 2009.

[24] M. Naushad, Z.A. AL-Othman, M. Islam, Adsorption of cadmium ion using a new composite cation-exchanger polyaniline Sn(IV) silicate: kinetics, thermodynamic and isotherm studies, Int. J. Environ. Sci. Technol., 10 (2013) 567–578.

[25] R.C. Bansal, M. Goyal, Activated Carbon Adsorption, Taylor and Francis, Boca Raton, 2005.

[26] M. Imamoglu, O. Tekir, Removal of copper (II) and lead (II) ions from aqueous solutions by adsorption on activated carbon from a new precursor hazelnut husks, Desalination, 228 (2008) 108–113.

[27] F. Xie, X. Lin, X. Wu, Z. Xie, Solid phase extraction of lead (II), copper (II), cadmium (II) and nickel (II) using gallic acid-modified silica gel prior to determination by flame atomic absorption spectrometry, Talanta, 74 (2008) 836–843.

[28] J. Anwar, U. Shafique, W. Zaman-uz, M. Salman, A. Dar, S. Anwar, Removal of Pb (II) and Cd (II) from water by adsorption on peels of banana, Bioresour. Technol., 101 (2010) 1752–1755.

[29] M. Moyo, L. Chikazaza, Bioremediation of lead (II) from polluted wastewaters employing sulphuric acid treated maize tassel biomass, Am. J. Anal. Chem., 4 (2013) 689–695.

[30] J.E.G. Mdoe, J.S.M. Makene, Removal of lead (II) ions from aqueous solutions using cashew nut shell liquid-templated thiol-silica materials, Bull. Chem. Soc. Ethiop., 28 (2014) 363–372.

[31] Almasi, M. Omidi, M. Khodadadian, R. Khamutian, M.B. Gholivand, Lead (II) and cadmium (II) removal from aqueous solution using processed, walnut shell: kinetic and equilibrium study, Environ. Chem., 94 (2012) 660–671.

[32] P. Chand, Y.B. Pakade, Removal of Pb from water by adsorption on apple pomace: equilibrium, kinetics, and thermodynamics studies, J. Chem., 2013 (2012) 1–8.

[33] F.J. Alguacil, P. Adeva, M. Alonso, Processing of residual gold (III) solutions via ion exchange, Gold Bull., 38 (2005) 9–13.

[34] R. Liu, P. Liang, Determination of trace lead in water samples by graphite furnace atomic absorption spectrometry after preconcentration with nanometer titanium dioxide immobilized on silica gel, J. Hazard. Mater., 152 (2008) 166–171.

[35] N. Lian, M. Chang, H. Zheng, S. Wang, Y. Cui, Y. Zhai, Application of dithizone-modified TiO_2 nanoparticles in the preconcentration of trace chromium and lead from sample solution and determination by inductively coupled plasma atomic emission spectrometry, Microchim. Acta, 151 (2005) 81–88.

[36] M. Ghasemi, Mu. Naushad, N. Ghasemi, Y. Khosravi-fard, A novel agricultural waste based adsorbent for the removal of Pb (II) from aqueous solution: Kinetics, equilibrium and thermodynamic studies, J. Ind. Eng. Chem., 20 (2014) 454–461.

[37] M. Naushad, Surfactant assisted nano-composite cation exchanger: development, characterization and applications for the removal of toxic Pb^{2+} from aqueous medium, Chem. Eng. J., 235 (2014) 100–108.